Sorption Kinetics of Poly(dimethylsiloxane) Networks: Diffusion of Polydisperse PDMS Blends

Ernst D. von Meerwall,*,†,‡ Travis Pryor,‡ and Vasilios Galiatsatos‡

Department of Physics and Maurice Morton Institute of Polymer Science, The University of Akron, Akron, Ohio 44325

Received May 30, 1997; Revised Manuscript Received December 5, 1997

ABSTRACT: Using the pulsed-gradient spin-echo NMR method, we have studied the diffusivity D of two highly polydisperse OH-terminated dimethylsiloxane blends (M_n = 15 900 and 26 400) in the melts and sorbed into networks made by linking the same material with tetraethoxysilane; the sol was carefully extracted before diffusant was added. Sorption took either 3 days for a 5% weight gain or 60 days for material weighing 5% of the network to be completely absorbed; samples were then equilibrated. Fitting an echo attenuation model based on M distribution to the data shows that for both systems the diffusion in the 3-day sample is several times faster and more broadly distributed than in either its melt or the 60-day sample, reflecting the tendency for smaller molecules to be sorbed more rapidly. This finding complements our earlier similar finding for sol extraction. The D distributions in the 60-day samples are identical in shape, but slightly lower in mean rate, to those in the neat melts, and both in excellent correspondence with the original M distributions, showing that the observed permselectivity is satisfactorily explained on the basis of sorption kinetics alone.

I. Introduction

The study of model elastomeric networks has elicited considerable interest in recent years,[1] taking advantage of the comparative simplicity of interpretation of their attributes given their well-controlled architectures.[2−4] Poly(dimethylsiloxane) (PDMS) has attracted particular attention in this respect; a number of careful studies of preparation, characterization, and basic properties have been reported.[3−7]

Even with the most careful attention to stoichiometry, synthesis of networks by chemical cross-linking usually is unable to incorporate all ingredients, leaving a small fraction (typically 2−5%) of unreacted (but not necessarily unreactive) unattached molecules, including unreactive cyclics,[7] branched fragments, and excess cross-linker, dispersed throughout the network. If the preparation is to serve as a permeable membrane, or more generally as host for diffusing molecular species, it is essential that these sol molecules be extracted before diffusant is introduced. In a previous study by this laboratory,[8] the efficiency of the standard extraction process for PDMS networks, based on repeated swelling−deswelling cycles, was studied with nuclear magnetic relaxation and the NMR-based pulsed-gradient spin-echo (PGSE) diffusion technique. It was found that the speed of extraction of sol components is strongly dependent on their molecular weight, with the largest (most slowly diffusing) sol molecules taking over 10 times longer to extract to the same trace concentration than the smallest sol molecules. These networks had been prepared from unimodal polydisperse ingredients or from bimodal blends of these. During the subsequent characterization of the extracted networks via PDMS sorbate diffusion measurements[9,10] it became clear that the polydispersity of the diffusant, and the time schedule of diffusant sorption, have a greater effect on the observed diffusivity and its distribution than do the architecture of these networks. Such sorption kinetics results are easiest to interpret if the network is only loosely cross-linked, that is, the molecular weight between chemical cross-links is not less than the entanglement spacing, and if the diffusant molecules are not entangled with the network.

In a recent report[11] the dependence of sorption rate on PDMS sorbate molecular weight in similar PDMS networks was examined via classical bulk sorption measurements, confirming a pronounced effect on the inferred (single or average) diffusion coefficient of PDMS having modest dispersity. In contrast, the present work benefits from the ability of the PGSE method to demonstrate permselectivity directly, by characterizing the full distribution of diffusion coefficients in polydisperse diffusants, not merely some average. Diffusion coefficients are related in a known way to the molecular weights of individual fractions in a polydisperse but homologous diffusant blend. Because the selectivity is pronounced even at small concentrations of a molecular species chemically identical to the network segments, and vanishes in the limit of infinite sorption time, it will be concluded that the mechanism of selectivity is simple diffusion kinetics alone, hence that it is unnecessary to invoke the existence of a cutoff imposed by solubility limits, e.g., chemical incompatibility.

The present work was motivated by issues raised in a predecessor study[12,13] using diffusants covering a wide range of molecular weights, absorbed by networks of diverse architectures. It was found that when polydisperse PDMS melts having molecular weights M_n near 700 or near 1500 were briefly sorbed into losely cross-linked, sol-extracted unimodal or bimodal PDMS networks, their diffusion rates decreased substantially by comparison with their own melts. However, diffusant melts with M_n near 15 900 or 26 400 sorbed into the same networks diffused several times faster than they did in their melts. Given the polydispersity of the diffusant batches and their short (1-day) exposure to the networks, this puzzling result is now seen to be a simple consequence of differential sorption kinetics.

† Department of Physics.
‡ Maurice Morton Institute of Polymer Science.

S0024-9297(97)00779-1 CCC: $15.00
Published on Web 01/22/1998

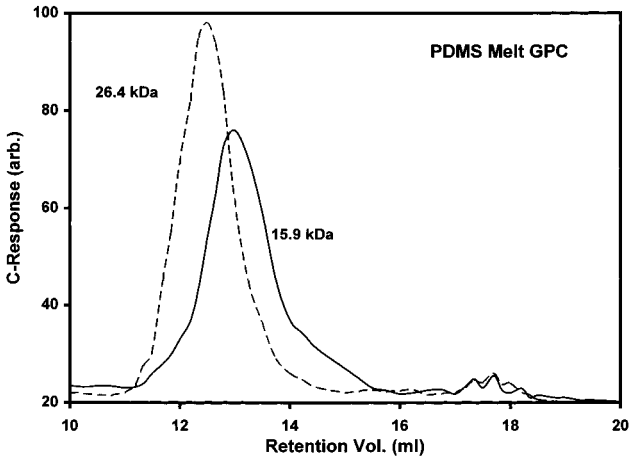

Figure 1. GPC traces in polydisperse PDMS melts of M_n = 15 900 and 26 400, showing the presence of small amounts of light material below $M = 700$.

This report is based on the MS Thesis of Travis Pryor (Polymer Science, University of Akron, 1996; unpublished). Preliminary reports of this and preceding work have been given.[12,13]

II. Experimental Section

A. Network Preparation and Characterization. Starting materials were linear, hydroxyl-terminated poly(dimethylsiloxanes) (Hüls America) of M_n = 15 900 and 26 400, used after extensive degassing. The GPC elution plots (Waters 410, toluene, columns HR-4E and -1) in the neat melts are shown in Figure 1. Both traces reveal the presence of a small amount of light material, usually attributed mainly to cyclic species,[7,14] amounting to 16.8 and 4.6 wt % below 10 000 for the lighter and heavier batches, respectively. The dispersity ratio M_w/M_n was found to be near 2 for both cases; exclusion of the low-M fraction at elution volumes above 16 mL (most likely mainly cyclic molecules[7] present as a result of ring−chain equilibrium[14]) reduced these ratios to 1.58 and 1.66, respectively. Because of their longer NMR T_2 relaxation times, measured on the same equipment used for the diffusion measurements (see below), these low-M fractions assume disproportionate importance in the interpretation of the PGSE diffusion spectrum, as will be seen below.

Networks were prepared by polycondensation reaction with stoichiometric amounts of the tetrafunctional cross-linking agent tetraethoxysilane aided by 1% of the catalyst tin(II) octoate (both supplied by Petrarch, Inc.). The liquid components were poured into Teflon-covered molds and kept at room temperature for 4 days under a dry N_2 atmosphere, producing cured sheets of thickness 0.10−0.15 cm. To extract the sol, the sheets were swelled in toluene, with fresh solvent supplied once a day for 5 days. To avoid rupturing the network, deswelling was accomplished gradually by staged replacement of toluene by methanol, until after 2 days the network had resumed its original size in 100% methanol. This process was followed by several days' evaporative drying in air. Weight losses obtained ranged between 2% and 5% for samples retained for study. Occasional greater weight loss was attributed to excess sol production due to departures from stoichiometry, and the offending samples were disqualified. The success of sol extraction (as well as solvent evaporation) was signaled by the absence of an observable proton spin-echo at 15 ms at room temperature. Glass transition temperatures were measured via DSC (DuPont DSC 2910) and showed that T_g is significantly lower in the networks than in the melts (−126.2 °C vs −123.5 °C for the 15 900 samples; −128 °C vs −124 °C for the 26 400 samples).

For simplicity of interpretation, each network was exposed to only one diffusant, the PDMS melt used in its preparation. Each of two sorption conditions was employed:

(a) A section cut from the central region of the extracted network sheet was immersed in the diffusant until the weight gain after removal of excess fluid from the surface was approximately 5%; at 30 °C this process consumed 3 days. The sample was allowed to equilibrate for at least 2 months in a drybox at 50 °C.

(b) The extracted sheet was presented with diffusant in the amount of 5% of its weight and then allowed to sorb completely at 30 °C. This process took approximately 60 days and was followed by the same equilibration as for the 3-day samples.

NMR samples were prepared by cutting circular disks from the films and stacking these in the bottom of a 7 mm o.d. NMR sample tube, which was then sealed under dry N_2 at atmospheric pressure. Network samples extracted but containing no sorbed diffusant, and samples of the neat PDMS melts, were also prepared for NMR/PGSE analysis.

B. NMR and PGSE Experiments and Interpretation. All NMR and PGSE experiments were carried out at 30 °C in the ^{1}H resonance at 33 MHz, on a modified Spin-Lock CPS-2 spectrometer adapted for large-pulsed-gradient operation in an iron-core electromagnet. For successfully extracted samples the transverse magnetization decay was nonexponential and reproduced published decay shapes for PGSE networks.[15] Network spin−spin relaxation times T_2 were found to be between 1.8 and 2.2 ms, whereas the single-exponential T_2 decays in melts and absorbed diffusants exhibited T_2 values between 18 and 45 ms. In specimens containing sorbed diffusant, a numerical decomposition[16] of the two-component relaxation decays resulted in cleanly separable components with relaxation times, respectively, near 2.6 and 20 ms or longer. This fact made it possible to conduct diffusant PGSE experiments using the principal spin-echo sequence 90°−τ−180°−τ−echo with τ = 25 ms without encountering an echo signal from the network.

PGSE experiments were conducted as described in detail elsewhere.[17−19] Briefly, a field-gradient pulse of magnitude G = 524 G/cm followed each of the two radio frequency pulses, thus keeping the gradient pulse spacing Δ equal to the radio frequency (rf) pulse spacing τ. The duration δ of the gradient pulses was adjusted in 20 or more steps from zero until the echo signal became unobservable or until δ reached 16 ms. A steady gradient of magnitude G_o = 0.8 G/cm was also applied to stabilize the echo signal and make its baseline easily accessible. The on-resonance echo signal after phase-sensitive detection was digitally acquired and its height $A(2\tau)$ numerically extracted and signal-averaged over up to 12 passes. Detector phase adjustments and gradient pulse-length corrections required at large δ were manually performed as described elsewhere.[18,19]

The measured echo attenuation patterns were subjected to detailed model analysis by an off-line code[20] DIFUS5 in its current version, which also produced echo attenuation plots $\log[A(2\tau,X)/A(2\tau,0)]$ vs X, where $X = (G\delta)^2(\Delta - \delta/3)$ with additional small terms[21] proportional to GG_o. In the presence of a single species with diffusion coefficient D, such a plot is consistent with a straight line[21] of zero intercept and slope $-\gamma^2 D$, where γ is the gyromagnetic ratio. Where more than one diffusing species is present, FT-PGSE experiments, permitting spectroscopic resolution of diffusing components on the basis of chemical shift differences, are of advantage. However, in cases such as the present polydisperse blends of intermediate M, chemical shift differences are unresolvable; also, the encountered diffusion coefficients may be too low to be confidently measurable with that method.

In the nonspectroscopic high-gradient version of the PGSE method employed here, a D distribution manifests itself as an upward concavity in the echo attenuation plots, arising from a linear superposition of component attenuations.[21] To extract information, this superposition must be modeled on the basis of known attributes of the sample, and the model fitted to the data by adjusting its parameters. Given the general lack of distinct features of the echo attenuation in such situations, the number of parameters optimized needs to be kept small, e.g., two or three. Our data-analysis code performed fits of

two such models to the same data; the contrast between the resulting interpretations will be instructive.

The effect of a log-normal diffusivity distribution on the diffusional echo attenuation may be satisfactorily discretized in terms, e.g., of nine components i centered on $i_C = 5$ and parametrized thus, with X defined as above:

$$\frac{A(2\tau,X)}{A(2\tau,0)} = \sum_i a_i \exp[-\gamma^2 D_i X] \tag{1}$$

where

$$a_i = B^{-1} \exp\left[-\left(\frac{D_i - \langle D\rangle}{\sigma_D}\right)^2\right] \qquad \sum_i a_i = B \tag{2}$$

and

$$\log D_i = \log \langle D\rangle + (i - i_C)\sigma_D/2 \tag{3}$$

The two adjustable parameters are $\langle D\rangle$ and σ_D; a provision for accommodating an additional, nondiffusing, echo component was not used here. The program reports the optimized (geometric) mean diffusivity log $\langle D\rangle$ and the D distribution expressed as the reduced standard deviation, $\sigma_D/\langle D\rangle$.

Alternately and preferably, the D distribution may be related directly to the M distribution of the diffusant. A comprehensive polydispersity model of this kind had been developed previously;[22] it generates an alternate discretized echo attenuation, implemented here with 11 components:

$$\frac{A(2\tau,X)}{A(2\tau,0)} = (1 - f_{fast})\sum_i a_i \exp[-\gamma^2 D_i X] + f_{fast} \exp[-\gamma^2 D_{fast} X] \tag{4}$$

where

$$a_i = w(M_i) \exp[-2\tau/T_2(M_i)] \tag{5a}$$

normalized to unity, with

$$T_2(M_i) = T_2(M_{ref})[M_i/M_{ref}]^b \tag{5b}$$

and with

$$b \cong -0.5 \tag{5c}$$

and

$$D_i = D(M_i) = D(M_{ref})[M_i/M_{ref}]^\alpha \tag{6a}$$

where

$$\alpha = -1\ (M_i < M_{ent}) \qquad \alpha = -2\ (M_i > M_{ent}) \tag{6b}$$

This model accounts for the differential T_2 weighting of the echo from different mass fractions, and the transition between Rouse-like diffusion ($D \sim M^{-1}$) below the entanglement onset point M_{ent} and reptational diffusion ($D \sim M^{-2}$) above that point. Free-volume effects in a single blend result only in an ensemble diffusivity adjustment without internal M dependence; tube renewal and chain reorganization effects are ignored.

This polydispersity-based model requires specification of an M distribution $w(M_i)$, which in the present case was provided in four versions: either as log-normal or Schulz−Zimm or Poisson distributions, each based on the M_w and M_n of the main GPC peak, or else by directly entering the digitized calibrated GPC trace of that peak. All of these versions produced essentially identical results when applied to our data. The model also contains an adjustable proportion of a single fast-diffusing component, accounting for the trace of light material known to be present in the diffusant. The diffusant

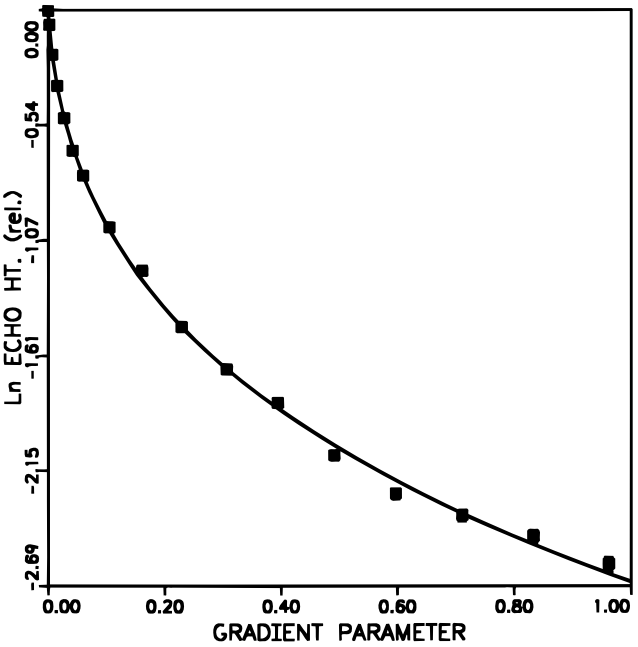

Figure 2. Diffusional echo attenuation (symbols) in a sample of 5 wt % of the 15 900 melt sorbed for 3 days into a network made from the same material. The abscissa variable is gradient parameter X defined in the text. The solid line represents the successful fit of eq 1 with eqs 2 and 3 to the data; fitted parameters are log $\langle D\rangle = -7.77$, $\sigma_D/\langle D\rangle = 2.8$.

$T_2(M_{ref})$ and the ensemble M exponent of T_2 were extracted approximately from the measured relaxation decays, and the entanglement onset point M_{ent} was derived from its literature value for monodisperse PDMS melts[23] with upward corrections[22] for the dilution of the entanglements by the lighter molecules in polydisperse melts. This correction is not operative for diffusant absorbed at small concentrations in a network. Where entanglement effects are present in our systems at all, they should be confined to a small trace of material at the highest tail of the M distribution and will have no more than a modest effect on the analysis (see below). There remain three adjustable parameters in the dispersity model: $D(M_n)$, D_{fast}, and f_{fast}, describing, respectively, the diffusion rate of molecules of $M = M_{ref} = M_n$, and the rate and fractional echo contribution of the rapidly moving light species.

While both interpretive models provided acceptable fits to the echo attenuation data, the polydispersity model was usually equal or superior in the quality of fit even when its additional adjustable parameter was accounted for. Its most important benefit, however, is the additional insight it confers into the origin of the permselectivity of the PDMS networks.

III. Results and Discussion

Figure 2 shows a sample diffusional echo attenuation plot, in the 15 900 diffusant as sorbed in its network for 3 days, together with the two-parameter fit of eq 1 with eqs 2 and 3. The echo attenuation plots in all specimens had a similar appearance but differed significantly in the values of the optimized parameters. The degree of upward concavity is a direct measure of the width of the reduced diffusivity distribution $\sigma_D/\langle D\rangle$ about the mean value $\langle D\rangle$. Figure 3 displays the results of the measurements for both sets of specimens in the form $\sigma_D/\langle D\rangle$ vs log $\langle D\rangle$. It is evident that the diffusivity in the 3-day samples is much more rapid on average, and somewhat more broadly distributed, than it is in the original melts. However, in the 60-day samples the diffusion rate returns to below their values in the melts, and the original D distribution is again approached. The

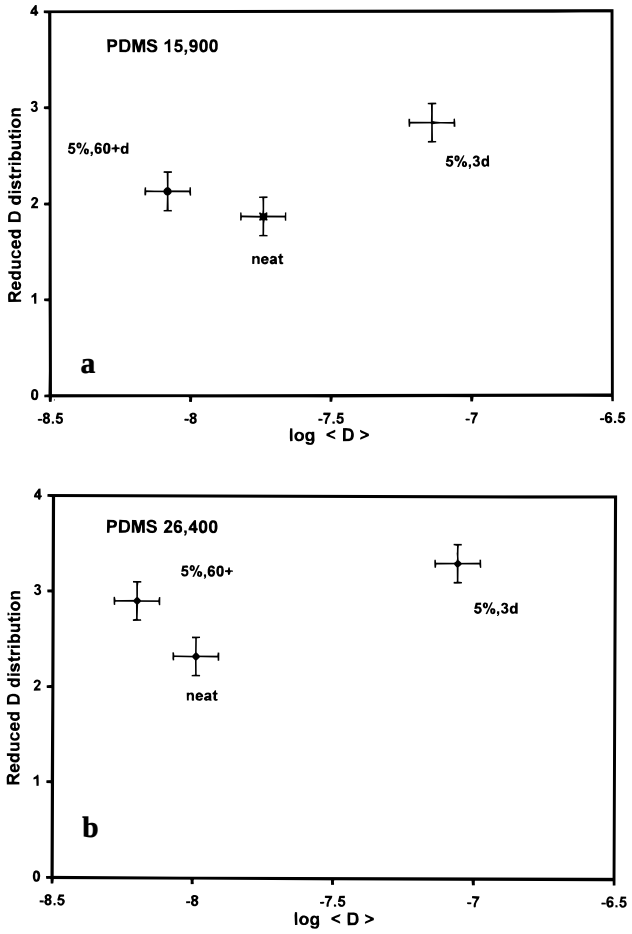

Figure 3. Results of the D distribution analysis in the melts (■), 3-day samples (+), and 60-day samples (●), for the 15 900 diffusant (a) and the 26 400 diffusant (b). The abscissa represents geometric mean diffusivity $\langle D \rangle$, the ordinate shows the reduced D distribution $\sigma_D/\langle D \rangle$ (see text).

apparent acceleration in diffusivity in the 3-day samples compared to the melts is startlingly large, amounting to a factor near four and near eight in the 15 900 and 26 400 diffusants, respectively. While these observations are clearly consistent with a sorption rate strongly dependent on molecular weight, a more detailed analysis is called for, both to improve the agreement between data and fit and to elucidate the operative mechanism.

The same echo attenuation data sets were therefore reanalyzed in terms of the polydispersity model, eq 4 with eqs 5 and 6. A sample echo attenuation plot with this model fitted is shown in Figure 4. The propensity of the smaller molecules in the polydisperse ensemble to dilute the entanglements in the remainder may be estimated by analogy with the effect of solvent, which raises M_{ent} above its undiluted value $M_{ent}°$. If v_P represents the volume fraction of polymer in solution,[24]

$$M_{ent} = M_{ent}°/v_P \tag{7}$$

In polymer blends the unentangled molecules may be regarded as diluent[22] for the entangled volume or weight fraction $v_P \gg w_P$, the latter to be derived from the M distribution above the entanglement onset point in the presence of dilution:

$$M_{ent} \approx M_{ent}°/w_P = M_{ent}°/\sum w(M_i) \qquad i(M_i > M_{ent}) \tag{8}$$

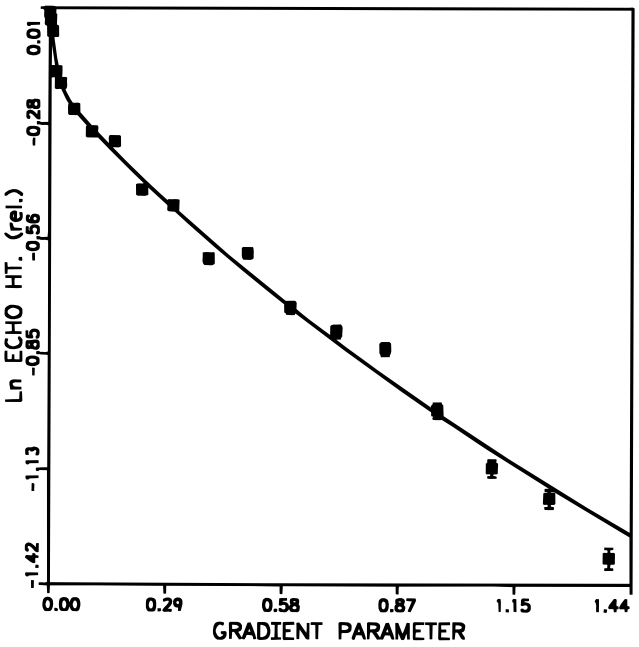

Figure 4. Diffusional echo attenuation (symbols) in a sample of 5 wt % of the 26 400 polydisperse melt sorbed for 60 days into a network made from the same material. The abscissa variable is gradient parameter X defined in the text. The solid line represents the successful fit of eqs 4−6 to the data; fitted parameters are $\log D_{fast} = -7.02$, $\log D(M_n) = -8.9$, and $f_{fast} = 0.16$.

This transcendental equation, discretized using 256 components from the GPC files, is solved numerically for M_{ent}.

These calculations showed that since M_{ent}(monodisperse PDMS melt) $\gg$ 19 000,[23] neither of our melts contain entangled molecules. In these cases the polydispersity model was set to adhere to pure Rouse scaling ($M_{ent} \rightarrow$ large) and produced excellent agreement with the data. Similar calculations for small concentrations of these diffusants in networks made of the same material (or in infinite-M melts) indicated that only the heaviest diluent fractions should become entangled with the network segments; M_{ent} was set to 25 000 for both the 3-day and the 60-day samples. Hence only the largest sorbed molecules (present mainly in the 60-day samples) are likely to be forced to reptate, slightly retarding them (eq 6b) by comparison with the melt. Trial fits of the model to both 60-day samples, in fact, showed that reptational scaling at the highest M is more probable than pure Rouse scaling.

The cause of the inferred modest decrease in mean diffusivity in the 60-day samples from the melt values, and its slightly broadened distributions, is now tentatively attributed to the reptational retardation of the largest molecules. On the other hand, the increase in $D(M_n)$ between the melts and the same diffusants in the 3-day samples cannot be related to reptation. Instead, it may be partly the result of the observed changes in T_g (a decrease of 3 or 4 deg from the melts to the networks). But this downward shift in T_g would also have raised rather than lowered $D(M_n)$ in the 60-day samples, or at least reduced its decrease. Thus we regarded the upward shift in $D(M_n)$ in the 3-day samples primarily as evidence of a downward shift of the main peak of the M distribution as a result of the preferential initial sorption of smaller molecules, that is, kinetic permselectivity. Such a shift has been described by

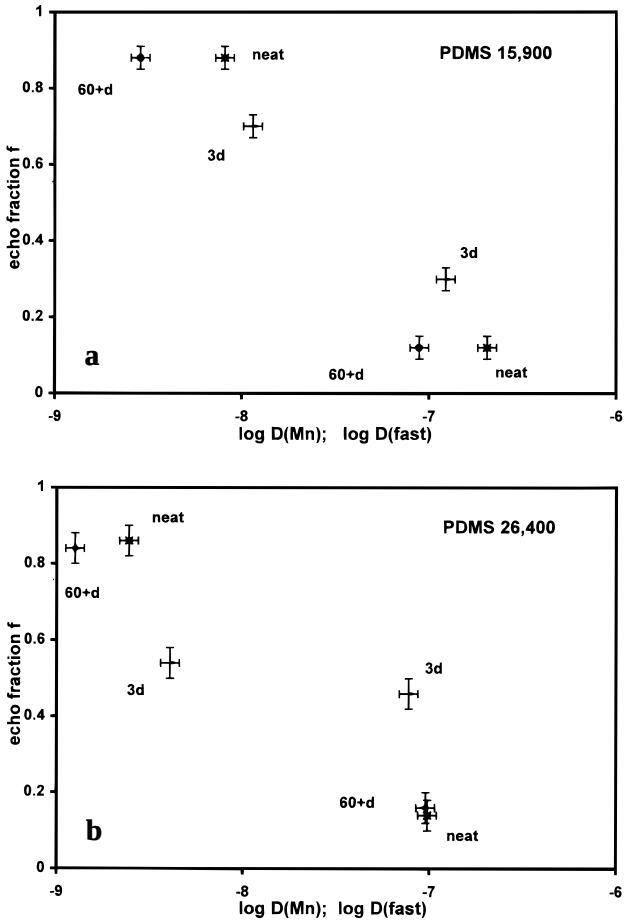

Figure 5. Results of the polydispersity analysis in the melts (■), 3-day samples (+), and 60-day samples (●), for the 15 900 diffusant (a) and the 26 400 diffusant (b). The abscissa represents the geometric mean diffusivity, log $D(M_n)$, for the disperse slower component (left) and single diffusivity, log D_{fast}, for the lighter species (right); the ordinate shows intensity fraction ($1 - f_{fast}$, left; f_{fast}, right) of the respective echo component, as discussed in text.

others.[11] In the present case its effect is minor by comparison with the differential sorption of the fractions corresponding to the widely separated major and minor GPC peaks, to be discussed next.

The results of the reinterpretation of the data with the polydispersity model are displayed for both sets of samples in Figure 5 in the combined form f_{fast} vs log D_{fast} and $(1 - f_{fast})$ vs log $D(M_n)$. This analysis assumes that the changes among each set of samples are confined to the relative amounts of heavy polydisperse blend vs light trace, with no substantial changes to the width (*i.e.*, dispersity ratio) of the *M* distribution of the high-*M* main component. (However, shifts in the main peak of the *M* distribution after sorption are accounted for in this model; see preceding paragraph.) The results are consistent with this assumption but also provide additional important insights. It is apparent that the diffusion coefficients of both the light and the main component undergo only modest changes during sorption, whether initial or equilibrium (see above). The central differences arise from the pronounced increase in the proportion of the light component in the 3-day samples, and the return in the 60-day sample to its value in the melt. This effect is significantly greater in the 26 400 sample set, in keeping with its greater *D* enhancement at 3 days as inferred earlier.

These observations constitute direct evidence of a strong *M*-selectivity of diffusant sorption in these materials, and for the hypothesis that this effect is mainly based on kinetics. While other contributing causes such as incompatibility or *M*-dependent solubility limits cannot be entirely excluded, our experiment was designed to reduce their likely influence. On the other hand, while the retardation of diffusion in the 60-day samples compared with the melt is evident, and the success of the fits tentatively points to its reptational origin, this is not emphatically apparent in Figure 5: entanglements do not become fully operative until well above M_{ent}, which in both cases is insufficiently greater than $M_{ref} = M_n$ to show a pronounced effect on the plotted $D(M_n)$. Hence the applicability of the reptation concept to our systems remains tentative and marginal.

The polydispersity model was not supplied with a value of the assumed single $M = M_{fast}$ for the light *M* fraction in the melts and diffusants. Such a value may be extracted from the fitted ratio of $D_{fast}/D(M_n)$ on the basis of M_n of the main GPC peak and the operative Rouse scaling law. Doing so results in M_{fast} between (350 ± 50) and (500 ± 60) in all cases, well within the minor low-*M* peak region of the GPC traces. Similarly, while f_{fast} exceeds the amount of light material detected by the GPC analysis, correction for the T_2 weighting of the echo signal strength (eqs 5a and 5b) with our estimated parameters (eq 5c) restores agreement at least semiquantitatively. Within the coarse stylization of this model, our analysis is, therefore, consistent.

IV. Summary and Conclusions

(1) PGSE experiments were performed on two polydisperse PDMS melts, and on networks made of these, cleaned of sol, and containing 5% of the same material either sorbed rapidly or exposed in equilibrium.

(2) The PDMS networks after extraction and drying were free of solvent and sol, as shown by NMR relaxation. After the diffusant was ingested, the PGSE echo attenuation contained no contribution from the network.

(3) The diffusional echo attenuation can be described heuristically in terms of a diffusivity distribution but is better understood on the basis of the diffusant's *M* distribution. That model interpretation is indifferent to the exact shape of the distribution but sensitive to its dispersity index and requires the assumption of an additional 5−10% of a light component of longer T_2.

(4) Detailed modeling shows that the parent *D* distribution seen in the melts is reproduced in network hosts after 60+ days of exposure; the uniform decrease in diffusivity is related to topological effects despite the slightly decreased glass transition temperature in the network. The rapid sorption of light fractions initially produces an increase in mean *D* combined with a wider *D* distribution.

(5) These results show that these PDMS networks are kinetically permselective to PDMS sorbate, *i.e.*, that the sorption rate is highly *M*-dependent.

(6) These findings complement and support our earlier findings on the kinetics of sol extraction in similar PDMS model networks.

The present study directly confirms the strong tendency of PDMS networks to separate sorbed molecules of similar chemistry but varying mass by virtue of pronounced differences in sorption rate, thus underlining the usefulness of such networks as candidates for semipermeable membranes for a variety of applications.

Further work in progress in this laboratory addresses diffusant sorption and permeation as affected by PDMS network cross-link density and its distribution, particularly in specimens prepared from bimodal blends. Supporting this effort is a separate study[25] to extract the network's full cross-link density distribution directly from the transverse NMR relaxation decay profile in the high-temperature regime.

Acknowledgment. The authors wish to acknowledge the extensive experimental groundwork for this study performed by J. Mantaseviphong and L. Sridhar. Several consultations with J. E. Mark and J. P. Kennedy on this and related topics were most helpful. The support of this work by the National Science Foundation, the American Chemical Society (Petroleum Research Fund), and the Ohio Board of Regents (Research Challenge program) are gratefully acknowledged.

References and Notes

(1) Mark, J. E.; Erman, B. *Rubberlike Elasticity: A Molecular Primer*; Wiley-Interscience: New York, 1988.
(2) Mark, J. E.; Sullivan, J. L. *J. Chem. Phys.* **1977**, *66*, 1006.
(3) Andrady, A. L.; Llorente, M. A.; Mark, J. E. *J. Chem. Phys.* **1980**, *73*, 1439.
(4) Mark, J. E. *Pure Appl. Chem.* **1981**, *53*, 1495.
(5) Mark, J. E. *Adv. Polym. Sci.* **1982**, *44*, 1.
(6) Andrady, A. L.; Llorente, M. A.; Mark, J. E. *J. Chem. Phys.* **1980**, *72*, 2282.
(7) Mark, J. E.; Llorente, M. A. *J. Am. Chem. Soc.* **1980**, *102*, 632.
(8) Galiatsatos, V.; von Meerwall, E. D. *Macromolecules* **1990**, *23*, 3551.
(9) Mantaseviphong, J. MS Thesis, Polymer Science, University of Akron, 1995 (unpublished). Mantaseviphong, J.; von Meerwall, E.; Galiatsatos, V. *Bull. Am. Phys. Soc.* **1993**, *38*, 348.
(10) Sridhar, L. MS Thesis, Polymer Science, University of Akron, 1996 (unpublished). von Meerwall, E.; Sridhar, L.; Galiatsatos, V. *Bull. Am. Phys. Soc.* **1996**, *40*, 2103.
(11) Mazan, J.; Leclerc, B.; Galandrin, N.; Couarraze, G. *Eur. Polym. J.* **1995**, *31*, 803.
(12) Pryor, T.; von Meerwall, E.; Galiatsatos, V. *Polym. Mater. Sci. Eng.* **1996**, *74*, 337.
(13) von Meerwall, E.; Pryor, T.; Galiatsatos, V. *Bull. Am. Phys. Soc.* **1996**, *41*, 676; **1997**, *41*, 1872.
(14) See: *Siloxane Polymers*; Clarson, S., and Semlyes, J. A., Eds., Ellis-Horwood-PTR Prentice Hall: Englewood Cliffs, NJ, 1993.
(15) See, for example: Sandakov, G. I.; Smirnov, L. P.; Sosikov, A. I.; Summanen, K. T.; Volkova, N. N. *J. Polym. Sci., Polym. Phys. Ed.* **1994**, *32*, 1585 and references therein.
(16) von Meerwall, E. D.; Thompson, D. *Comput. Phys. Commun.* **1983**, *31*, 385.
(17) von Meerwall, E. D.; Burgan, R. D.; Ferguson, R. D. *J. Magn. Reson.* **1979**, *34*, 339.
(18) von Meerwall, E. D.; Ferguson, R. D. *J. Appl. Polym. Sci.* **1979**, *23*, 877. See also: Pacanovsky, J.; Kelley, F. N.; von Meerwall, E. *J. Polym. Sci., B: Polym. Phys.* **1994**, *32*, 1339.
(19) von Meerwall, E. D.; Kamat, M. *J. Magn. Reson.* **1989**, *83*, 309.
(20) von Meerwall, E. D.; Ferguson, R. D. *Comput. Phys. Commun.* **1981**, *21*, 421.
(21) Stejskal, E. O.; Tanner, E. J. *J. Chem. Phys.* **1965**, *42*, 288.
(22) von Meerwall, E. D.; Palunas, P. *J. Polym. Sci., Polym. Phys. Ed.* **1987**, *25*, 1439.
(23) Ferry, J. D. *Viscoelastic Properties of Polymers*, 3rd ed.; Wiley: New York, 1980.
(24) Berry, G. C.; Fox, T. G. *Adv. Polym. Sci.* **1967**, *5*, 261.
(25) Apanius, C.; von Meerwall, E. *Bull. Am. Phys. Soc.* **1995**, *40*, 1482.

MA9707796